

COB-2023-2396
**EFFECTS OF THE GTAW TRIPLE ELECTRODE PROCESS ON
AUTOGENOUS WELDING OF CARBON STEEL PLATES**

Tiago Ballmann de Campos

Alisson Fernandes da Rosa

Federal University of Santa Catarina - UFSC

tiago.ballmann@grad.ufsc.br

alissonaula@gmail.com

Emanuel Silva da Rosa

Federal University of Santa Catarina - UFSC

emanuelrosa8@gmail.com

Mateus Barancelli Schwedersky

Federal University of Santa Catarina - UFSC

m.barancelli@ufsc.br

Régis Henrique Gonçalves e Silva

Federal University of Santa Catarina - UFSC

regis.silva@labsolda.ufsc.br

Abstract. *The GTAW (Gas Tungsten Arc Welding) is a process that uses an electric arc between a non-consumable electrode and the piece to be welded. Despite being widely used and making a high quality finish, the conventional method using pure argon is often labeled as low productive. As the travel speed increases, so must the current, therefore the generation of defects such as humping is imminent. Thus, some versions of GTAW uses more than one electrode as an alternative to minimize the humping effect, such as the present study, which uses a version with three tungsten electrodes in a triangular arrangement. To characterize multielectrode welding, this study does an overall analysis of the process, in which were performed autogenous over plate welding tests with 1, 2 and 3 electrodes, respectively. In addition, the performance of the process was evaluated under three different welding speeds, reaching up to 1,5m/min welding speed on every tested condition. The penetration and microhardness profiles were also evaluated. The results show that the use of multiple electrodes is, in fact, effective in reducing humping. A considerable decrease on the penetration values was also identified, especially for higher welding speeds. Moreover, it was possible to validate the experimental equipment (welding torch) for triple electrode welding, extending the application range of TIG welding. Thus, the present work shows that the use of TIG can be diverse, and even more, considering the number of electrodes. The process using three electrodes, which showed the lowest penetration, for example, has potential for coating applications or welding thin plates, where these characteristics are highly desired.*

Keywords: TIG, multicathode welding, high-speed welding, humping.

1. INTRODUCTION

Among the various welding processes, some stand out in specific areas and therefore are preferred over others. The GTAW (Gas Tungsten Arc Welding) process uses an electric arc between a non-consumable electrode and the work piece to be welded. This arc is protected by an atmosphere of inert gases, usually Argon, Helium, or a mixture of the two. The process is widely used in industry and has the ability to generate high quality finishes, however the conventional method using pure argon is often labeled as low productive because its travel speeds are typically lower than the PAW (Plasma Arc Welding) process' and its wire feed speed is lower than those presented by the GMAW (Gas Metal Arc Welding) process, for example.

Furthermore, the low productivity is related to defects that arise in the process. As the travel speed increases, so must the current, but due to the high stagnation pressure, the generation of defects such as humping is imminent, as explained by Lancaster (1984), that "molten metal may be blown out of its proper location".

According to Mendez (1999), humping is an irregular surface formed by a series of rounded protuberances, found when the welding current and speed exceed a threshold value. Schwedersky (2015) explains that this phenomenon occurs because the arc pressure works pushing the liquid metal from the front of the weld pool to the back. As the travel speed

risers and the melt velocity exceeds the welding speed, the weld pool is exposed to a lower temperature and premature solidification can be identified, therefore creating a non-continuous solidification on the weld bead that is typically a sequence of craters and protuberances alternating between them.

Thus, new versions of the TIG process that present more than one electrode are emerging as an alternative to minimize the adverse effects of using high currents, aiming to eliminate the appearance of humping. In this context, giving continuity to the research already developed by Schwedersky (2015), Souza (2021) and Rosa (2023) in relation to the TIG processes with coupled arcs, where the necessary devices for the process were developed, and the morphology, behavior and electrical interaction between arcs were analyzed, besides identifying and establishing the sharpening angle and distance between the electrodes as main parameters for the process. Thus, enabling the present work, which uses a version with three tungsten electrodes on a triangular arrangement to evaluate the effects of welding speed on the weld bead.

2. MATERIALS AND METHODS

A general analysis about the TIG process was made, aiming to characterize the multi-electrode welding. The welding source employed was an “IMC MTEdigitec 600” for the frontal electrode, and a “Digiplus A7 450” for the electrodes on the back, each electrically isolated. The mechanical structure of the welding torch is schematized in Figure 1.

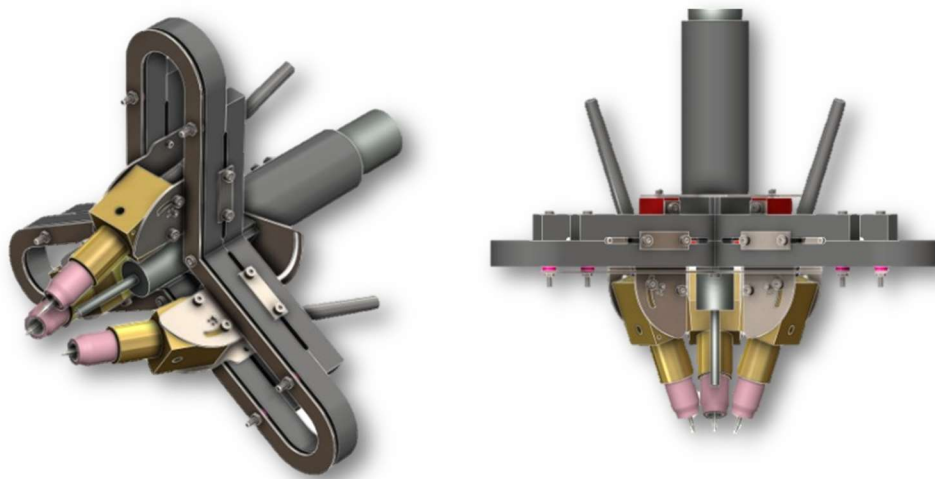


Figure 1: Multicathode torch (Rosa, 2023)

Autogenous welding tests were performed varying the number of electrodes at different travel speeds, each weld bead was divided into 3 sections with a change in travel speed from 0.5 to 1 and 1.5m/min, respectively, without interrupting the process. Also, to ensure robustness and reproducibility of the results, each electrode configuration was tested three times. The electrodes travel angle was 40° with flat tip.

In table 1, below, a matrix of the experiments can be seen, each experiment was done using a fixed current of 300A split evenly among the number of electrodes used.

Experiment	Section A (0.5 m/min)	Section B (1 m/min)	Section C (1.5 m/min)
1		1 electrode	
2			
3			
4		2 electrodes	
5			
6			
7		3 electrodes	
8			
9			

Table 1: Experiments

Welding was performed at flat welding position on 3/8" AISI 1020 steel plates, the tests were performed with the parameters as shown in Table 2.

Parameter	Value
I (A)	300
Arc length (mm)	3
Arc Voltage Control (V)	Disabled
Gas type	Argon
Preflow time (s)	7
Gas (L/min)	30
Electrode diameter (mm)	3.2
Truncation diameter (mm)	1
Electrode distance (mm)	1,5

Table 2: Welding parameters

The microhardness was measured using “VH1102 Micro Hardness Tester - From BUEHLER/WILSON”, and the metallography panoramic pictures taken on “Binocular microscope Carl Zeiss model Axiolab”. The penetration and microhardness profiles were also evaluated.

3. RESULTS AND DISCUSSION

In sequence from welding, the morphology of the beads was analyzed, as shown in Figure 2.



Figure 2: Top view of the weld beads

As the number of electrodes increases, the decrease of the humping effect in the bead is noticeable. In the tests performed, with two electrodes the humping is no longer found for travel speeds of 0.5 m/min and 1 m/min, and occurs only for 1.5 m/min. Using three electrodes humping can't be found but the bead is much narrower. In this context, taking into account that the increase in the number of electrodes increases the area and decreases the arc pressure, it is possible to assume that for higher currents, there will be a range of currents in which the humping will be identified with two electrodes but will be minimal with three. This effect can also be seen by the growth of the HAZ (heat-affected zone), which is proportional to the current density. After welding, the macrograph of each section was made, as shown in Figure 3:

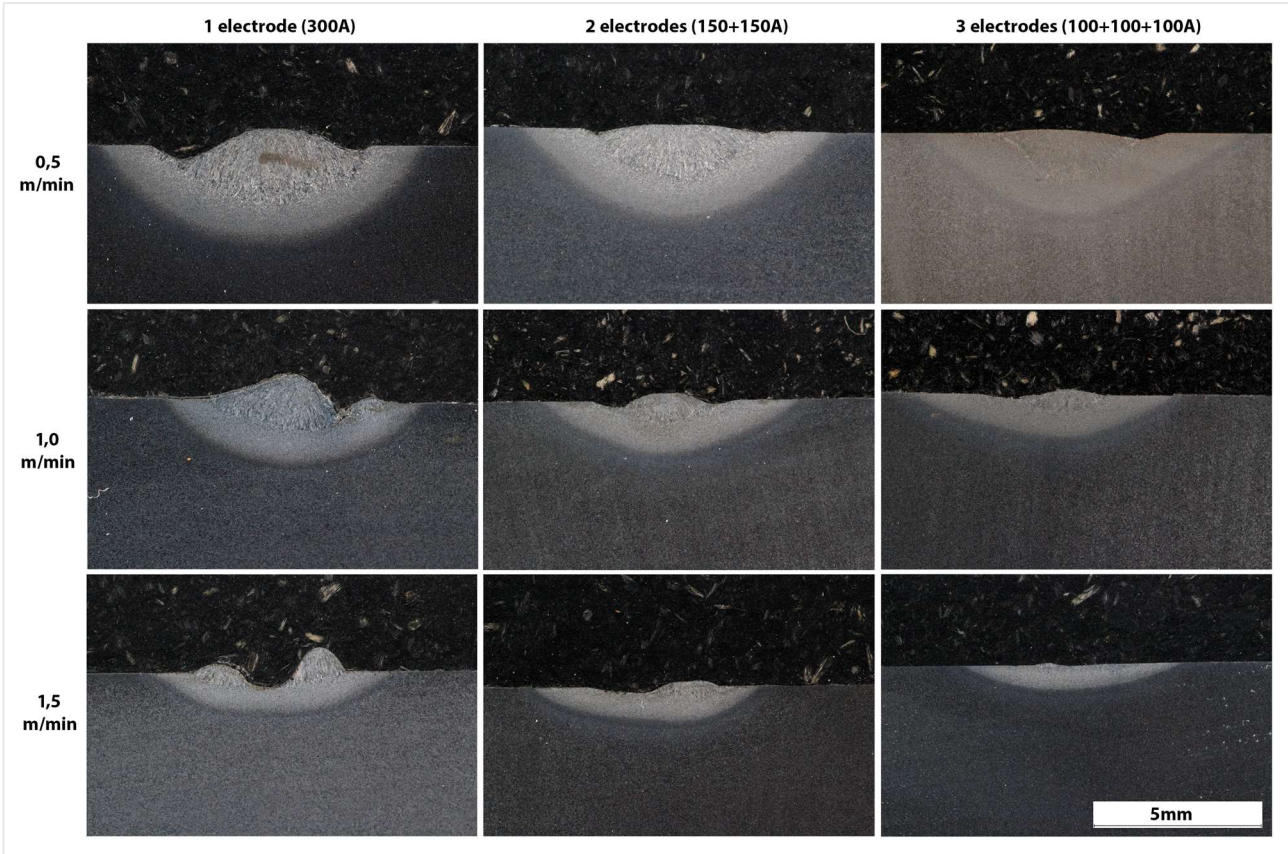


Figure 3: Weld bead macrographs

The Table 3, below, compares the penetration, dilution and area of the weld metal zone values for each of the sections with 1, 2 and 3 electrodes, respectively.

Section	1A	1B	1C	2A	2B	2C	3A	3B	3C
Penetration (mm)	2.157	1.638	1.170	1.678	0.938	0.670	1.573	0.680	0.300
Diluição (mm ²)	86.450	64.230	61.506	92.278	83.272	83.226	95.348	86.441	97.151
Weld metal zone (mm ²)	8.524	4.104	2.377	5.439	1.907	1.240	4.106	1.121	0.702

Table 3: Weld metal zone analyses

From Table 3, three graphs were made. In Figure 4, the graph shows the diminishment of the WMZ (weld metal zone) area according to the increase in number of electrodes. The increase in travel speed also showed the same effect. The tendency line of the graph for penetration in Figure 5 also shows it to be proportionally inverse to the number of electrodes.

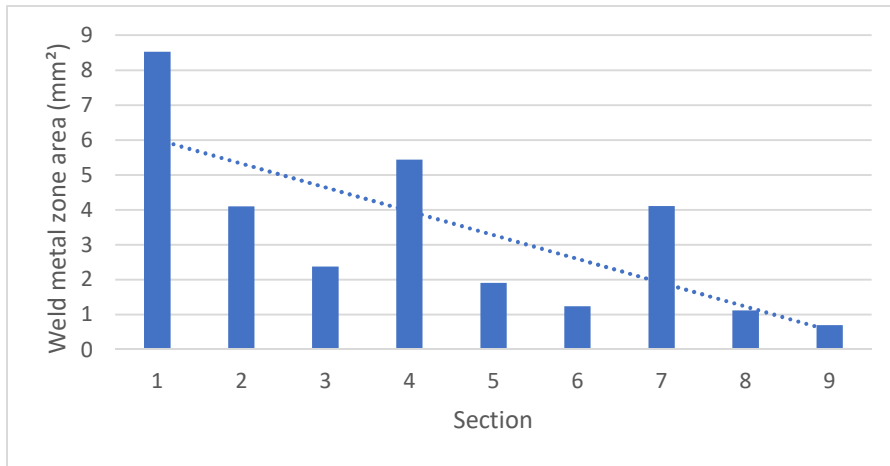


Figure 4: Weld metal zone area by section

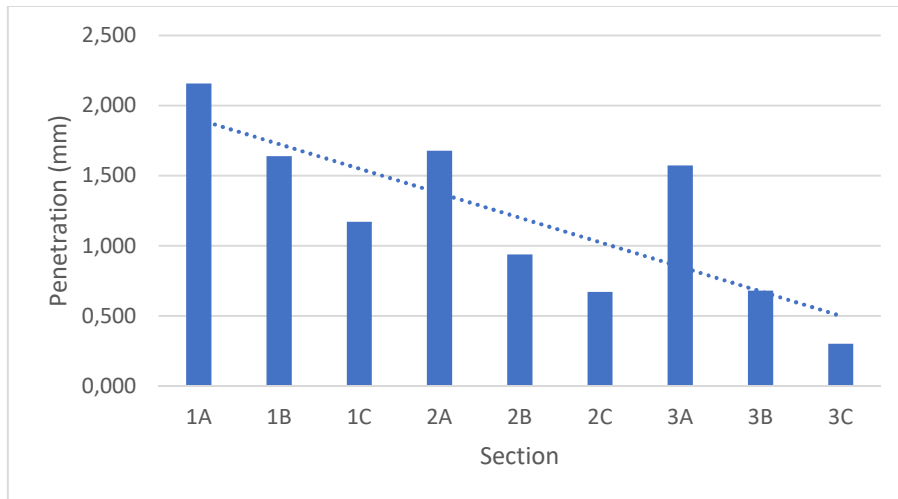


Figure 5: Penetration by section

Opposite from the previous cases, in Figure 6 it is notable that the dilution increases with more electrodes.

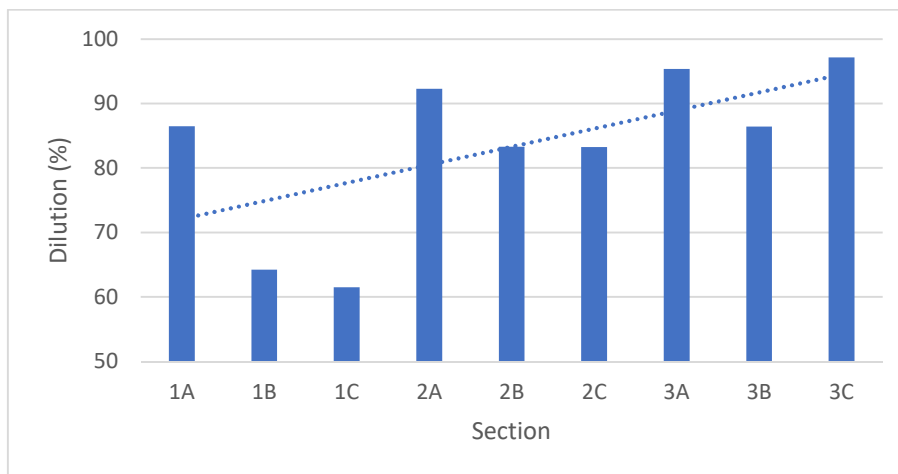


Figure 6: Dilution by section

3.1 Microstructure analysis

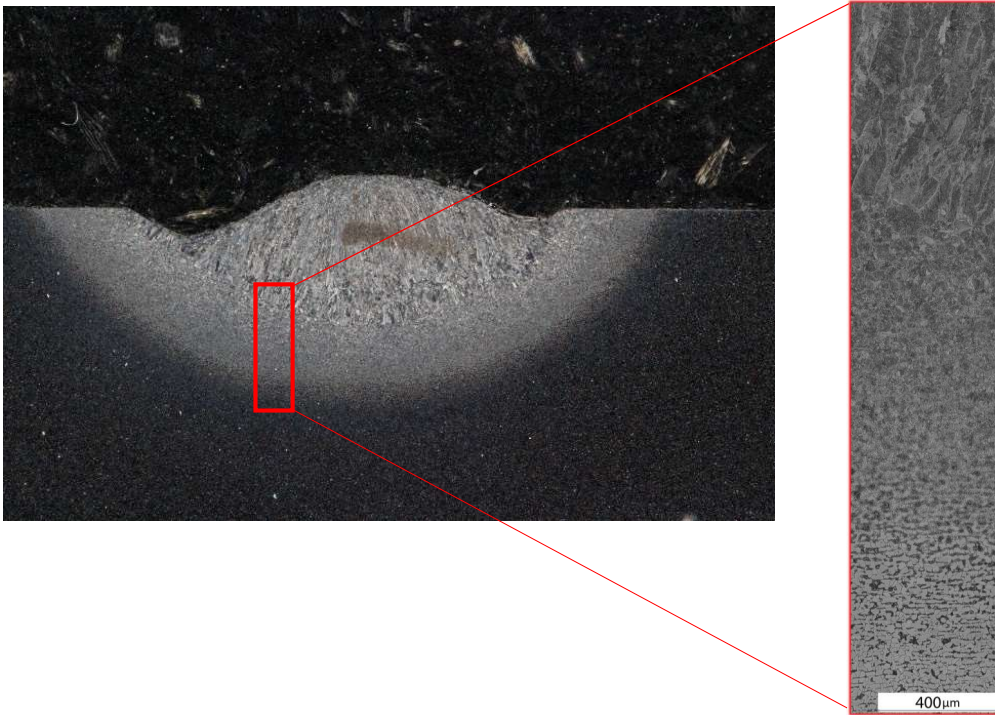


Figure 7: Microstructure profile of section 1A

The microstructure images (Figure 7) show the progression of the weld metal zone and the heat-affected zone over the base metal. The tests performed used 1020 steel with no filler material, so predictions of the microstructure can be made using the iron-carbon phase diagram.

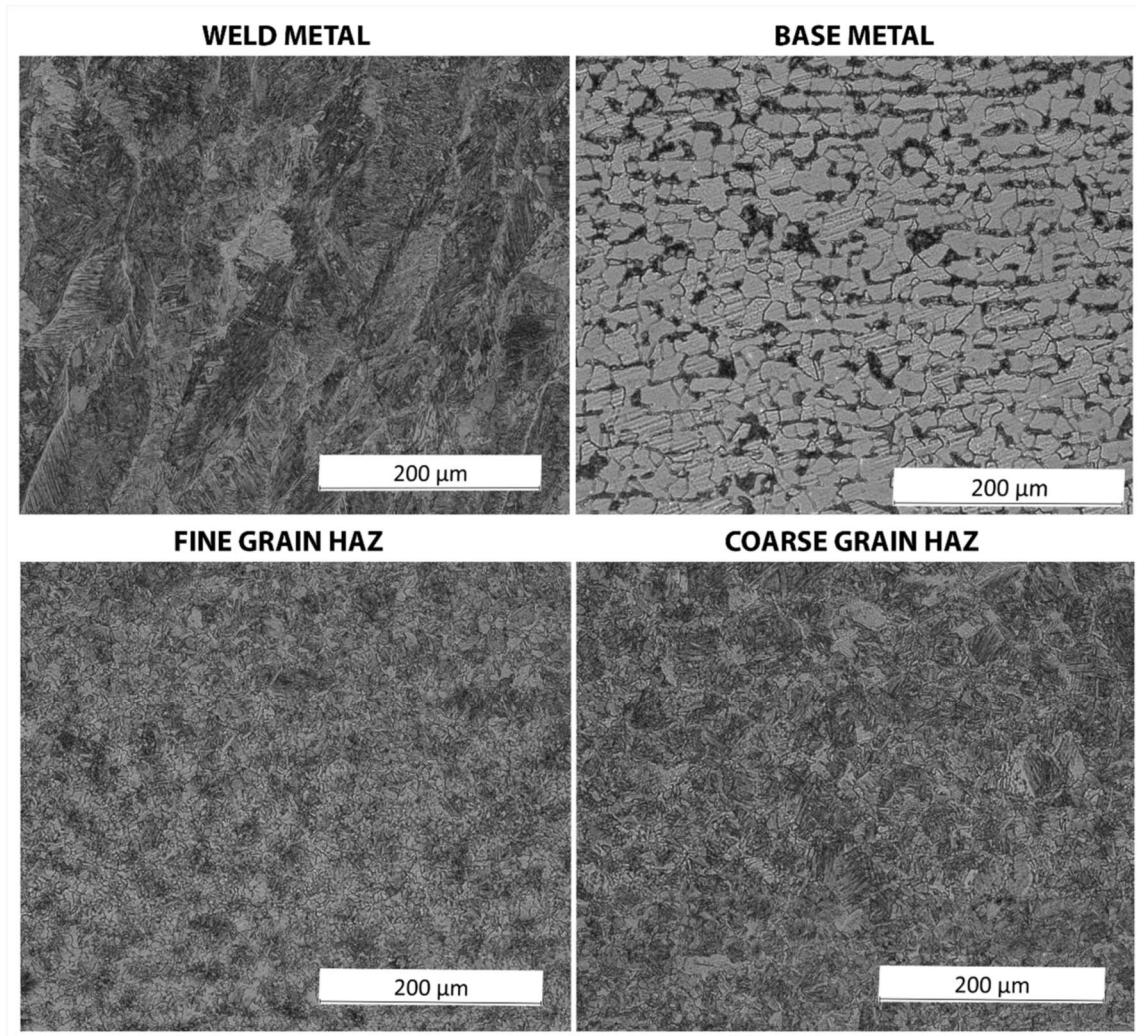


Figure 8: Micrograph of section 1A

The microstructure of 1020 steel (0.2% C) is composed of two phases, ferrite and pearlite. In figure 8, ferrite can be identified in the macrograph of the base metal as the white region, and pearlite as the dark spots.

The weld metal zone (top left corner in figure 8) presents a different microstructure, the grains of ferrite are columnar, which due to the longer period in heated state had intense grain growth. The “spikes” that grow inwards from the grain boundary resemble the widmanstatten plate ferrite, generated by either the propagation of an unstable interface or a sympathetic nucleation according to Phelan & Dippenaar (2004).

At the beginning of the HAZ grain growth is also identified, resulting in a coarse grain zone. According to Modenesi (2012), this effect occurs because the region is exposed to temperatures higher than 1200°C, creating bigger austenitic grain boundaries, the final microstructure also has higher hardness values and is less ductile. As the HAZ progresses towards the base metal, more heat has been dissipated and less austenitization has occurred, creating a fine grain HAZ due to recrystallization.

According to Callister (2016), the pearlite present in the microstructure of low-carbon steels is a lamellar mixture of ferrite and cementite and forms a single grain, called colonies. These layers are created due to the diffusion of carbon after welding when the austenitic metal cools and separates into ferrite and cementite. Cementite (Fe_3C) appears as the dark phase, it is a hard and brittle phase that can significantly increase the strength of the steel. Despite the fragility of cementite alone, this phase will be beneficial to the material, without the adverse effects typically associated with the presence of martensite. It is worth noting that martensite formation would be negligible due to the low amount of carbon.

3.2 Microhardness analysis

In Figure 9, the microhardness profiles of each welding bead from travel speeds of 0.5m/min were combined.

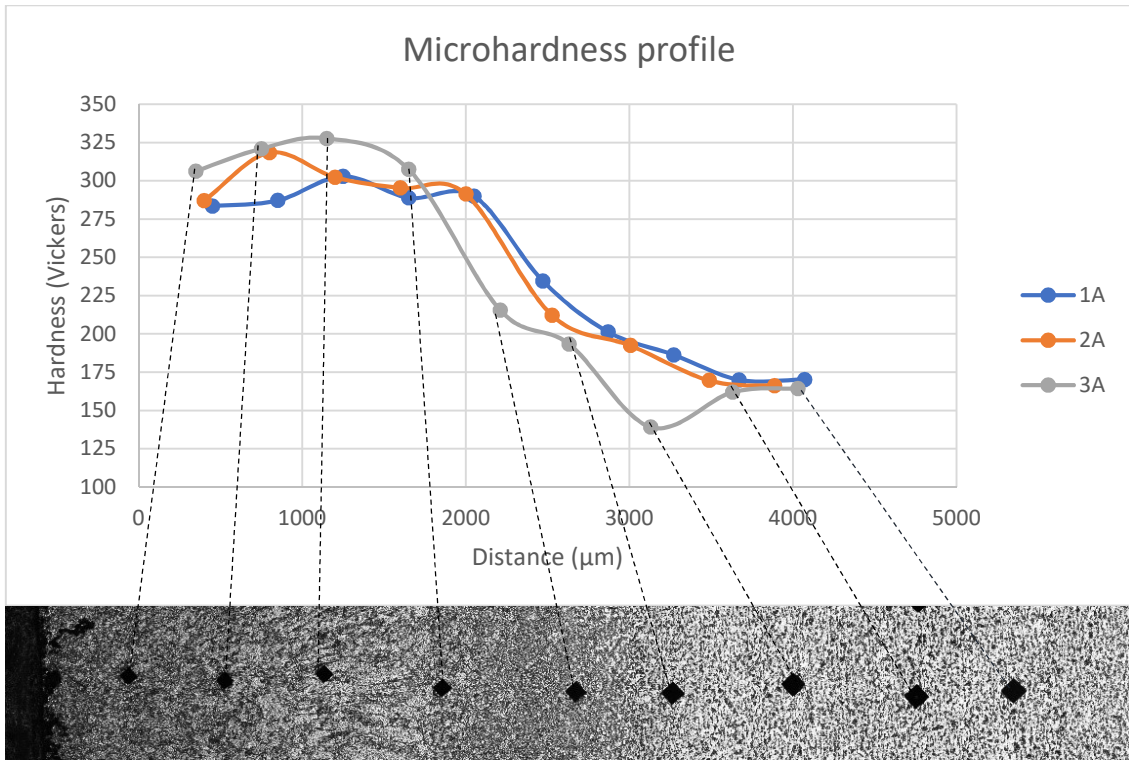


Figure 9: Microhardness profile

Next, in Figures 10, 11 and 12 the microhardness profile of the A sections (welding speed of 0.5m/min) is represented for each pass versus the advancement of the fusion zones and HAZ, at the background of each graph is a representation of the indentations made by the tests.

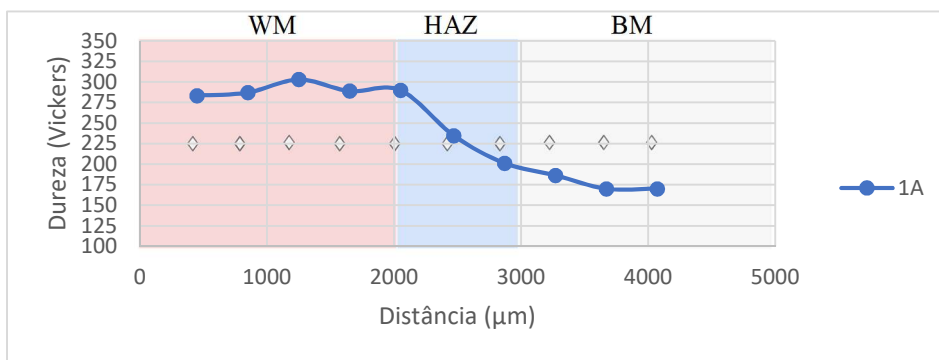


Figure 10: Microhardness profile of section 1A

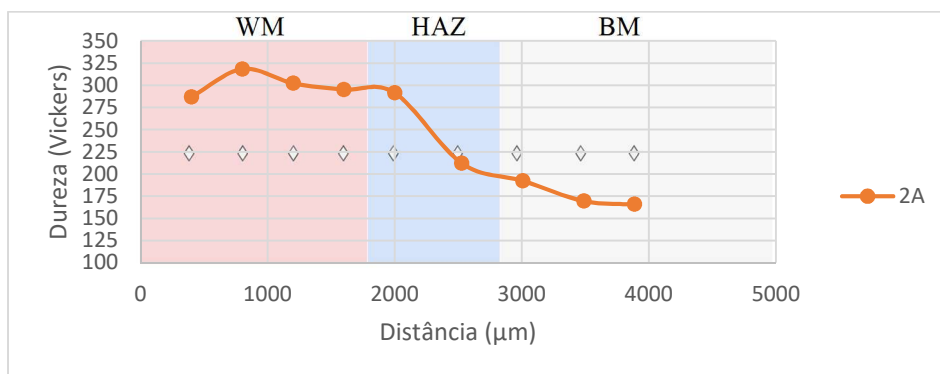


Figure 11: Microhardness profile of section 2A

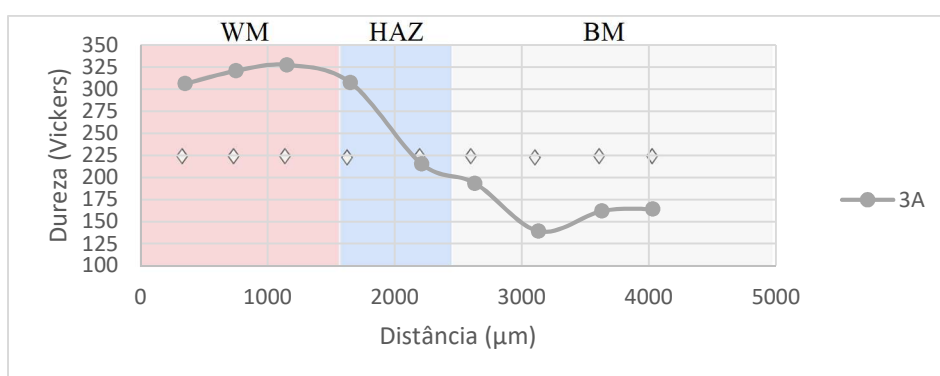


Figure 12: Microhardness profile of section 3A

As the number of electrodes increases, it is noticeable the decrease in the weld metal zones. When analyzing the graph from left to right, in each zone there is a drop in measured microhardness values, this effect continues until the standard microhardness value of the base metal is reached (approximately 170 HV 1). The lower penetration at welding generates narrower zones in the graph, and thus, anticipates the drop in microhardness.

4. CONCLUSIONS

The results suggest that the use of more than one electrode is, in fact, effective in reducing defects. The three electrode process was an effective measure against humping arising on high travel speeds. A considerable decrease in penetration values was also identified, especially for higher welding speeds. Moreover, it was possible to validate the experimental equipment (welding torch) for welding with three electrodes, extending the range of application of the TIG process. Thus, this work shows that the applications of the TIG process can be diverse, especially considering the number of electrodes.

At high travel speeds, which presented the lowest dilution, for example, presents potential for coating applications or welding thin plates. In coating processes, the low penetration could also be an advantage. Furthermore, for future studies, it is also plausible to evaluate the effects of wire addition.

5. REFERENCES

- CALLISTER JR, William D, RETHWISCH, David G. *Ciência e engenharia de materiais – uma introdução*. 9. ed. Rio de Janeiro: LTC, 2016. Chapter 10
- MENDEZ, P. F.; NIECE, K. L.; EAGAR, T. W. Humping Formation in High Current GTA Welding. *International Conference on Joining of Advanced and Specialty Materials II*. Cincinnati-OH; 1999.
- MODENESI, P. J., MARQUES, P. V., SANTOS, D. B. *Introdução à Metalurgia da Soldagem*. Belo Horizonte: UFMG, 2012. Chapter 6.
- Phelan, Dominic and Dippenaar, Rian, "Widmanstatten ferrite plate formation in low-carbon steels" (2004). Faculty of Engineering and Information Sciences - Papers: Part A. 2662
- ROSA, A. F. Technological Insights Into The TIG Multicathode Welding. In: *12th Brazilian Manufacturing Engineering Congress – COBEF, 2023*.
- SCHWEDERSKY, M. B. *Estudo e Desenvolvimento do Processo TIG Duplo Eletrodo*. UFSC. 2015.

SOUZA, M. dos A. Desenvolvimento de bancada experimental e estudo da morfologia do arco elétrico no processo de soldagem TIG com três eletrodos. UFSC. 2021 ZANINI, J. B. Understanding of Humping Based on Conservation of Volume Flow - Peter Berger*, Helmut Hügel, Axel Hess, Rudolf Weber, Thomas Graf. Physics Procedia 12 (2011) 232–240.
J.F. Lancaster 1984 Physics in Technology 15 73

6. RESPONSIBILITY NOTICE

The author(s) is (are) the only responsible for the printed material included in this paper.